Saturable absorber for ring fiber lasers on the base of coupler coated by CNTs

Dmitry A. Korobko[a*], Dmitry A. Stoliarov [a], Pavel A. Itrin [a], Valeria A. Ribenek[a], Artem V. Sysa[b], Yury P. Shaman[b] and Andrei A. Fotiadi[a,c]

[a]Ulyanovsk State University, L. Tolstoy str., 42, 432017, Ulyanovsk, Russia; [b]Scientific-Manufacturing Complex "Technological Centre", Shokin Sqr., 1, Zelenograd, 124498, Moscow, Russia., [c]University of Mons, blvd. Dolez 31, Mons, B-7000, Belgium.

ABSTRACT

We report on a new method for fabrication of saturable absorbers for operation in ring fiber lasers as a mode-locking element taking advantages of the manufacturing technologies of fiber couplers and microfiber tapers coated with carbon nanotubes. It is demonstrated in the experiment that the transmittance of the fabricated saturable absorber increases with an increase of the input radiation power. Also, we have shown that the fabricated saturable absorber enables generation of picosecond soliton pulses in ring fiber laser configuration.

Keywords: saturable absorber, carbon nanotubes, fiber coupler, fiber laser.

1. INTRODUCTION

Currently, ultrashort pulse lasers are effectively used in various fields of everyday life. They are exploited both in research and services delivered to mass consumers, e.g., medicine, cosmetology, etc. Owing to a multiple consumer appeal, fiber lasers definitely benefit over all mode-locked lasers. Small size, relatively low cost, convenient fiber output, and high beam quality make them attractive for a large number of applications [1-10]. To deliver ultrashort pulses, a fiber laser configuration comprises either active [11], or passive mode–locking element with an incorporated saturable absorber [12, 13]. In recent years some hybrid options have been developed also [14-18]. Low-cost and reliable passive mode-locking, mainly exploited in ultrashort pulse laser sources, enables generation of the pulses with a pulse duration much shorter than the modulator switching time [19].

Saturable absorbers (SA) are the key elements of passively mode-locked lasers. They conventionally could be divided in two types: artificial and natural SAs. Saturable absorbers based on Kerr lensing [20], nonlinear mirror [21], and nonlinear polarization rotation (NPR) belong to the first group [22-24]. NPR saturable absorbers are mainly used with fiber laser configurations. Although the lasers based on such SAs are easy-to-use, they are environmentally sensitive and require adjustment to initiate lasing that limits their practical application. Semiconductor mirrors (SESAM) [25-27] or SAs based on topological insulators [28], graphene [29], and carbon nanotubes (CNT) [30-32] belong to the group of natural SAs. Besides low cost and ease of use, the CNT technology is advantageous over the SESAM technology in ability to modulate transmittance thus simplifying laser circuits based on ring fiber cavities. As a result, CNT-based saturable absorbers have replaced SESAMs in a number of fiber laser applications [33-36].

The principle methods of CNT-based SAs fabrication are deposition of CNTs on a film, fiber end face [37, 38], chemically etched d-shape fiber [39] or micro-taper obtained by thermal drawing of a standard fiber [40, 41]. Each of the methods has specific limitations and drawbacks. In particular, the film method significantly limits the radiation power in the cavity [42], the d-shape technology requires special fiber structure and it's rather complicated [39]. In this work, we focus on the microfiber method of SA fabrication, in which CNTs are deposited on a fiber thermally drawn up to the diameters compared with the radiation mode area [40, 43]. The evanescent field based CNT SA, manufactured by this method, has an advantage over the schemes using CNTs deposited on a film or fiber end face enabling generation of higher pulse energy and peak power. Such absorbers are simple to manufacture and easy-to-use, but suffer specific drawbacks. Due to a small diameter of taper waist region (~ 10 μm), when coated with CNTs at a high concentration or from a liquid phase, SA experiences high losses induced by the fiber deformation. The same restrictions impede the uniform distribution of CNTs over the microfiber surface. In addition, fiber tapers are sensitive to environment that can deteriorate their performance characteristics. To overcome these problems, the use of polymer composites has been proposed [44]. Along with additional protection of the microfiber, a polymer with a low refractive index (e.g., 2,2,2-

---

[*]korobkotam@rambler.ru

trifluoroethyl methacrylate (PTFEMA), n = 1.42) provides the effective distribution of nanomaterial on its surface and prevents formation of agglomerations, thereby reducing SA losses from estimated 50% down to 15% [45, 46].

In this work, we push forward development of the microfiber method for fabricating CNTs-based SAs. For this purpose, the fiber couplers commonly used in fiber circuits are employed. The fabrication process includes simultaneous thermal drawing of two parallel fibers down to the diameters close to the mode field size followed by fusion [47]. The fibers fused into a coupler are elongated enough to enable interaction of radiation with the CNT film on their surface and saturable absorption. Since fiber coupler is a mechanically stronger structure than a standard microfiber, it is able to provide a simplified technology of CNT-film deposition in a polymer composition while maintaining a high saturation absorption coefficient. In particular, simplification of the technology within this approach allows using less precise (e.g., aerosol) methods of nanomaterial coating, which, in its turn, enables deposition of larger CNT-volumes and optimization of SA properties.

2. MANUFACTURING OF A CNT-COATED COUPLER

Single-walled CNTs (SWCNT) used for coupler coating have been synthesized by the electric arc technology at the Institute of Problems of Chemical Physics, the Russian Academy of Sciences (Chernogolovka, Russia). An average diameter of SWCNTs is 1.5 nm. Inset in Fig. 1 (a) shows the absorption spectrum of the used CNTs in the wavelength range 550-2400 nm. SWCNTs have been subjected to multistage liquid-phase treatment in order to obtain stable and homogeneous suspensions in a solution of 2,2,2-trifluoroethyl methacrylate (Sigma-Aldrich No. 373761) in N-methylpyrrolidone subsequently used as a matrix for SA structure [48, 49]. Fig. 1 (a) shows the Raman spectra of the CNT structure before and after liquid-phase treatment. The spectra are obtained using LabRAM HR Evolution spectrometer at an exciting radiation wavelength of $\lambda_0 = 514$ nm. The Raman spectrum analysis shows that CNTs demonstrate predominantly semiconductor conductivity [50]. Comparison of the intensities of spectrum lines D and G (I_G/I_D) gives estimations to the value L_a describing the length of defect-free regions in the CNT structure [51, 52]:

$$L_a(nm) = 2.4 \cdot 10^{-10} \lambda_0^{\,4} \frac{I_G}{I_D} \qquad (1)$$

The estimation shows that after a multi-stage liquid-phase treatment, the size of defect-free regions is reduced, on average from 504 nm down to 62 nm.
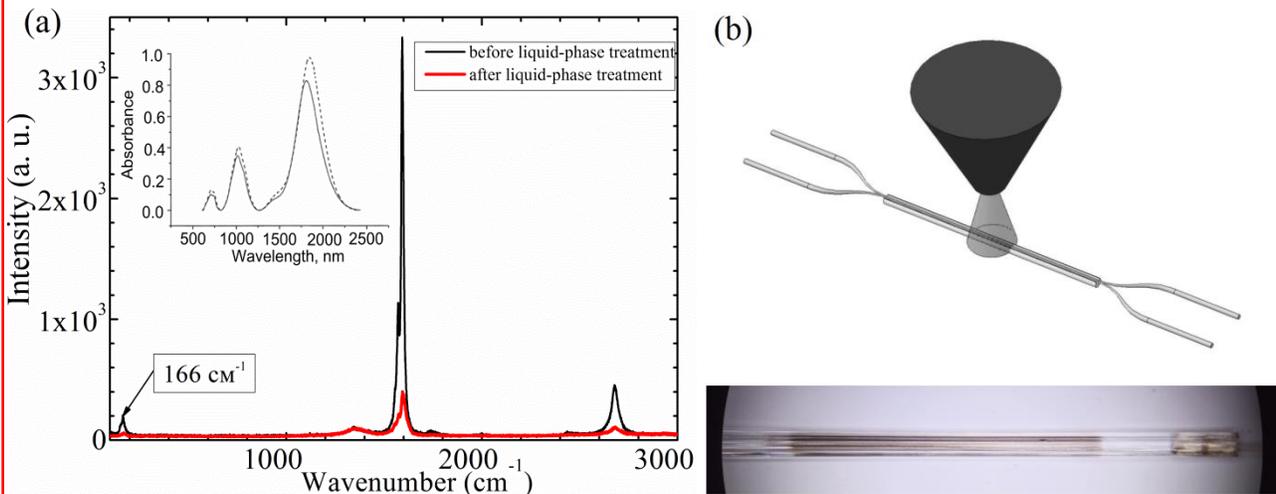

Fig. 1. (a) Raman spectra of the CNT structure before and after liquid-phase treatment. Inset: The CNTs absorption spectrum. (b) Schematic of CNT deposition on the fiber coupler surface and a photo of the fused fiber coupler covered by CNTs in a quartz cell.

The 60/40 fiber coupler from the standard SMF fibers without cladding has been fabricated using the standard thermal fusion technology with a hydrogen torch for fiber couplers and WDM. The taper waist length, where the fiber cladding diameter decreases from 125 μm down to values close to the mode field diameter (9-10 μm), is $l = 18$ mm. The intrinsic loss of the manufactured coupler is $L_0 = 0.5$ dB. Before coating with CNTs, the coupler is placed in a quartz cell and

SPIE USE: _____ DB Check, _____ Prod Check, Notes:

glued to keep its waist fixed in a suspended position. CNTs are deposited from the aerosol of the prepared suspension in a nitrogen atmosphere with infrared heating of the coupler surface up to 50 ° C. After a 10 min deposition, the CNTs cover almost the entire length of the coupler. (Fig. 1 (b)) and the coupling ratio has changed to 49/51 due to penetration of the CNT-polymer suspension into the coupler structure.
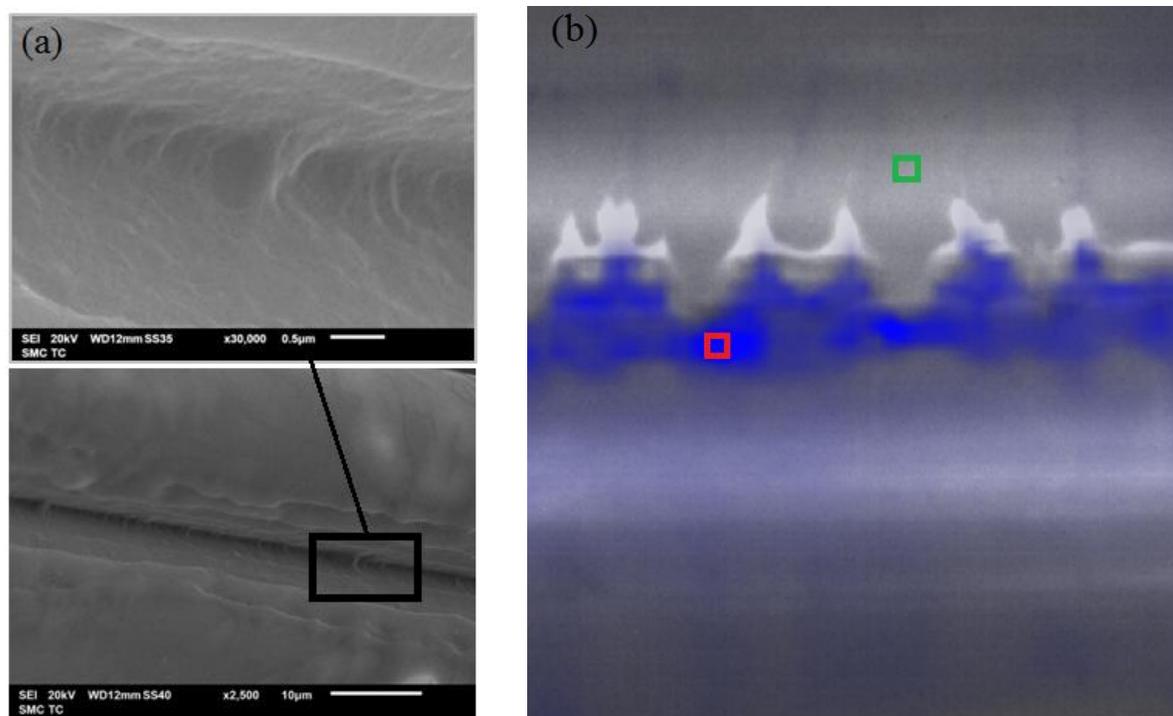

Fig. 2. (a) SEM image of CNTs located between optical fibers. (b) Image of the coupler irradiated at 514 nm to get the distribution of SWCNT G-band intensity. Red and green squares correspond to the maximum and minimum G+ peak intensity (1590 cm^{-1}), respectively.

The image of the coupler waist region after CNT deposition taken by JEOL JSM-6010PLUS SEM is shown in Fig.2 (a). Also, the coupler sample has been studied by the Raman spectroscopy methods. In Fig. 2 (b), the distribution of CNT G-band intensity (1570-1595 cm^{-1}) is shown in the coupler waist. The distribution is recorded under laser irradiation of the sample at the wavelength of 514 nm and power of 1 mW. The acquisition step and durations are 1 μm and 0.1 s, respectively. The blue color intensity is proportional to the G-band intensity that, in its turn, is proportional to a number of CNTs. The points corresponding to the minimal and maximal CNT G-band intensities are marked in Fig. 2 (b). One can see that CNT bundles are concentrated mainly in the trench between two tapered fibers forming the fused coupler.

3.   MEASUREMENT OF THE SATURABLE ABSORPTION

The key characteristic of a SA is the dependence of losses it introduces on the intensity (or power) of the input radiation. If the losses decrease with the input power, SA can be used for mode-locking and pulse generation through positive optical feedback in the laser cavity it provides [23].

A standard configuration shown in Fig. 3 (a) has been employed to evaluate characteristics of the fabricated CNT-coupler used as a saturable absorber [51, 52]. A soliton laser operating at the wavelength of $\lambda = 1.55$ μm delivers pulses with the duration of ~ 1.4 ps and repetition rate of 3.84 MHz. A variable attenuator is used to control the power at the input of the manufactured CNT-coupler. Recording the power levels at all outputs of the experimental setup allows us to determine the transmittance of the CNT-coupler. The experimental results shown in Fig. 3 (b) describe the CNT - coupler transmittance as a function of the average power at the coupler input.
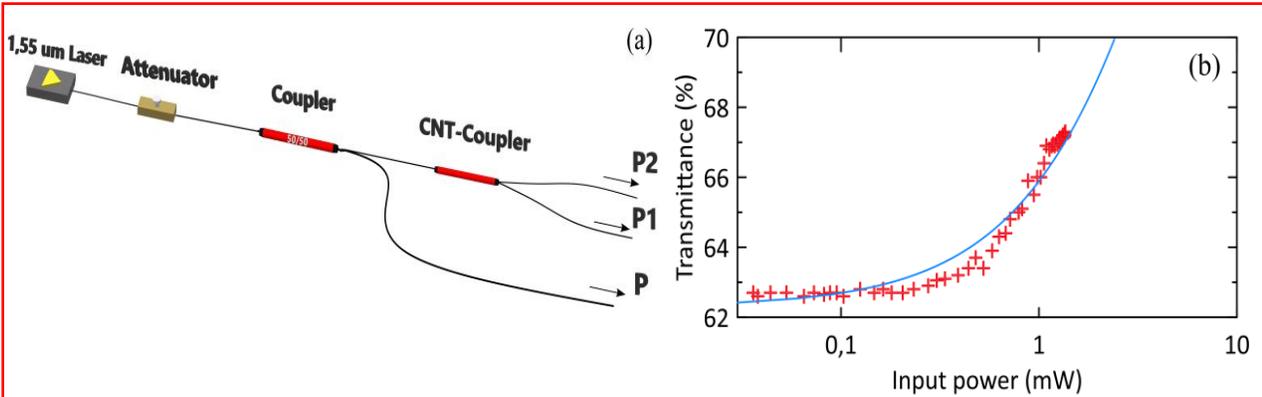
Fig. 3. (a) Schematic of the experimental setup for measuring saturable absorption in a CNT - coupler. (b) Experimentally measured coupler transmittance as a function of the radiation power at the input. Solid blue line is an approximation of the obtained data by dependence (2) for the parameters: $\alpha_0 = 18\%$, $P_S = 500$ Вт, $\alpha_{NS} = 19\%$.

A change in the average power corresponds to a change in the peak power P_0 of the input soliton pulse (a simple estimation shows that 1 mW of the average power corresponds to $P_0 \approx 93$ W). Therefore the same experimental results show the transmittance of the CNT - coupler as a function of the peak power at the coupler input. One can see a reliable increase of the coupler transmittance with an increase in the pulse peak power that is the key property of SA important for mode-locking. The experimentally measured depth of SA modulation is ~ 4.5%. However, the experimental data have been limited by the output power of the soliton source corresponding to its transition to the multipulse generation mode. Some theoretical estimations can be made using SA model with instantaneous relaxation time. In this model, the absorption coefficient α of SA, depending on the radiation power P, is expressed in terms of the modulation depth α_0, saturation power P_S, and the value of unsaturated losses α_{NS}:

$$\alpha = \frac{\alpha_0}{1 + P/P_s} + \alpha_{NS}.$$

For the soliton pulses with the sech^2 envelope and peak power P_0, the SA transmittance T with instantaneous relaxation can be expressed through the parameter $s = P_0/P_S$ [35] as:

$$T = \frac{\alpha_0}{\sqrt{s(1+s)}} \text{atanh}\left(\sqrt{\frac{s}{1+s}}\right) + 1 - \alpha_{NS}. \tag{2}$$

These estimations give the modulation depth of the fabricated SA $\alpha_0 > 10\%$ at high enough saturation power $P_S > 350$ W. Fig. 3 (b) shows an approximation for relation (2) at $\alpha_0 = 18\%$, $P_S = 500$ Вт, $\alpha_{NS} = 19\%$.

4. STUDY OF CNT-COUPLER IN A RING FIBER LASER SCHEME

To study the mode-locking provided by the fabricated CNT - coupler, the coupler has been incorporated into a standard Er-doped fiber ring laser. The ring laser configuration (Fig. 4) contains no polarization-sensitive elements, so mode-locking through the nonlinear polarization rotation is prohibited in this scheme.
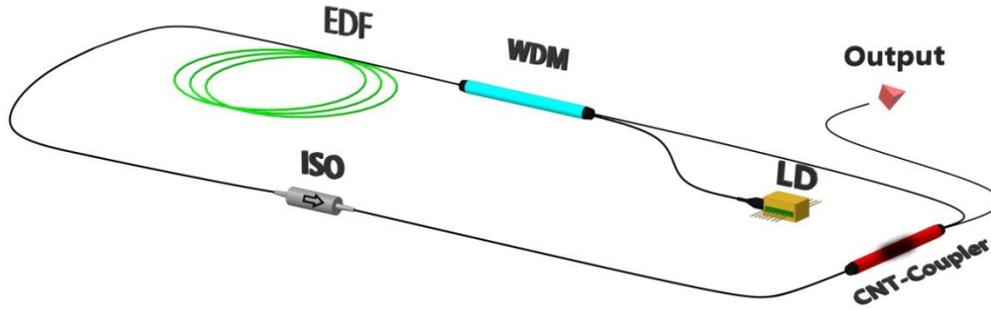
Fig. 4. Experimental set-up of a fiber laser with CNT- coupler. LD is the pump diode, WDM is the wavelength-division multiplexer, EDF is the Er-doped fiber, ISO is the fiber isolator.

The laser cavity contains 0.5 m of Er-doped EDF-150 fiber with a normal dispersion of 19 ps^2/km at 1550 nm. All other elements are connected by an SMF-28 fiber with a dispersion of −20 ps^2/km at 1550 nm. The total cavity length of 10.5 m corresponds to a fundamental repetition rate of 19.07 MHz, while the total cavity dispersion is ~ −0.196 ps^2. The configuration is pumped by a laser diode with a wavelength of 975 nm and a maximal power of 550 mW. The output radiation is emitted through a CNT- coupler. The laser self-starts to operate in a pulsed mode at a pump power of 50 mW, while the output power is 1.7 mW. The single-pulse lasing operation is maintained with the pump power levels up to 165 mW, whereas the output power increases to 3.3 mW. The optical spectrum and pulse autocorrelation describing this mode are shown in Fig. 5.
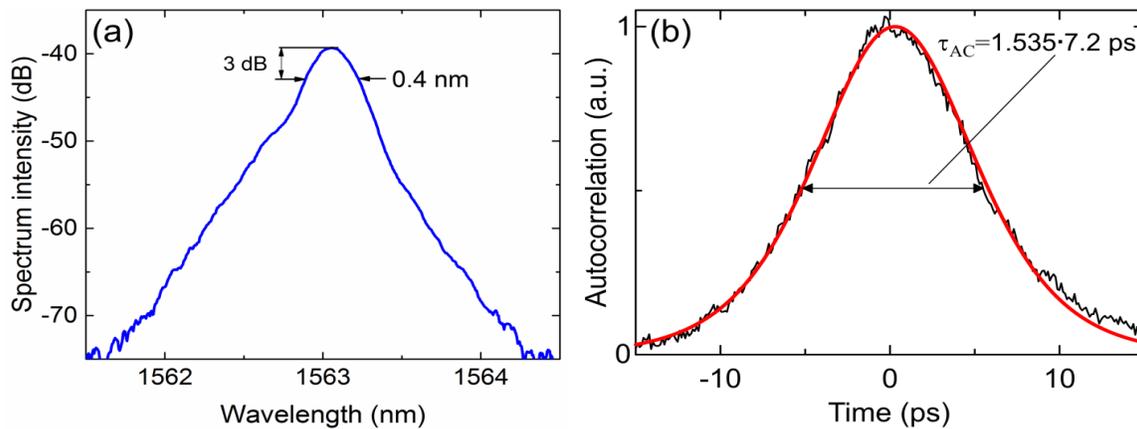

Fig. 5. (a) Optical spectrum and (b) autocorrelation of a laser pulse generated in mode-locked ring fiber laser with a CNT-coupler. The solid red line describes the $sech^2$ envelope.

Despite an incomplete suppression of sidebands leading to a noticeable spectrum asymmetry, the pulse envelope shape is close to $sech^2$, while the product of the pulse duration (~ 7.2 ps) and pulse spectrum width (~ 0.4 nm) is TBW ~ 0.355, justifying that a pulse is close to a spectrally limited soliton. Fig. 6 shows the radiofrequency spectrum of the laser recorded with a resolution of 100 kHz. One can see that a stable spectrum comprising harmonics of the fundamental ring cavity mode exhibits no parasitic modulation and filtering. The signal-to-noise ratio for the fundamental (first-order) harmonic gets the level of >60 dB and then slowly decreases with the harmonic number thus highlighting a high quality of the laser signal.
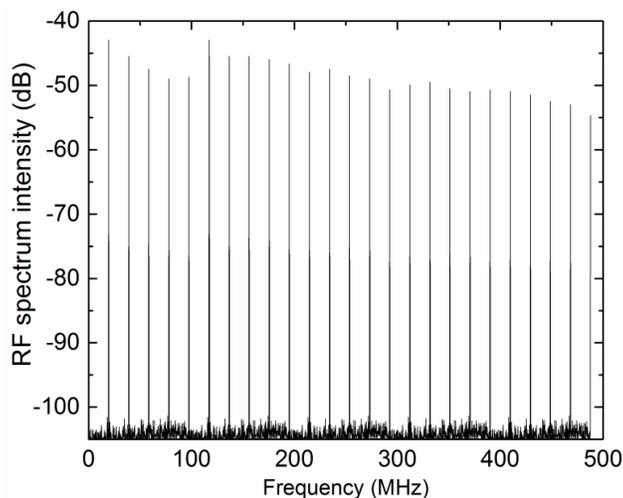
Fig.6. Radiofrequency spectrum of mode-locked ring fiber laser with a CNT- coupler.

5. CONCLUSIONS

In this study, we propose a new fabrication method of SA for mode-locking of the ring fiber lasers taking advantages of the manufacturing technologies of fiber couplers and tapers coated with carbon nanotubes. The proposed method develops the technology of microfiber tapers coated with CNTs, but simplifying it, in particular, allowing usage of less complicated methods of nanomaterial deposition. The simplicity of the proposed CNT- coupler technology is in the use of widely available materials and standard laboratory equipment.

A standard experiment on measurement of the transmittance has confirmed that the fabricated sample of a CNT- coupler demonstrates the main property of SA, i.e. its transmittance increases with an increase in the peak power of the input pulse. The performed estimations show that this sample has a sufficiently high modulation depth ($> 5\%$), however, its saturation power is also quite high ($P_s > 350\,\mathrm{W}$). Noteworthy, the use in the experiment of a pulsed source with the peak power of soliton pulses $P_0 < 150\,\mathrm{W}$ has not resulted in a change or degradation of the CNT- coupler characteristics.

The experiment has confirmed applicability of the CNT- coupler for mode-locking in a soliton ring fiber laser. In the reported laser configuration, the nonlinear polarization rotation effect on mode-locking is eliminated. The performance of the laser is not perfect, however, we have shown that the fabricated sample possesses the SA characteristics suitable for generation of picosecond soliton pulses. Specifically, the proposed technology is able to maintain generation of picosecond pulses in configurations with a relatively low Q-factor of the cavity (the output ratio of the used CNT-coupler is close to 50/50). In the future, the SA parameters will be further improved through the use of a CNT-coupler with lower output coefficients (10 or 5%) to increase the laser cavity Q-factor and generate pulses of much shorter duration. Also, we will upgrade the proposed technology using the improved SA characteristics (reduction of the saturation power and unsaturated losses), high quality CNTs fabrication and composition parameters (quantity, geometry) of nanomaterials. Promising methods of CNT deposition such as magnetron-sputtering-deposition method, photonic crystal fiber assisted deposition and so on [53-58] could be considered as more accurate and controllable fabrication process of CNT coated fiber couplers. We suppose that the optimizing device could be applied not only in the telecommunication range but also in other important spectral regions (for example, in 2 μm range).

REFERENCES

[1] Shi, W., Fang, Q., Zhu, X., Norwood, R. A., and Peyghambarian, N., "Fiber lasers and their applications," Applied optics, 53(28), 6554-6568 (2014).

[2] Fermann, M. E., and Hartl, I., "Ultrafast fibre lasers," Nature photonics, 7(11), 868-874 (2013).

[3] Droste, S., Ycas, G., Washburn, B. R., Coddington, I., and Newbury, N. R., "Optical frequency comb generation based on erbium fiber lasers," Nanophotonics, 5(2), 196-213 (2016).

[4] Keller, U., "Recent developments in compact ultrafast lasers," Nature, 424(6950), 831-838 (2003).

[5] Gattass, R. R., and Mazur, E., "Femtosecond laser micromachining in transparent materials," Nature photonics, 2(4), 219-225 (2008).

[6] Preda, C. E., Fotiadi, A. A., & Mégret, P., "Numerical approximation for Brillouin fiber ring resonator. *Optics express*, *20*(5), 5783-5788, (2012).

[7] Fotiadi, A. A., Antipov, O. L., and Mégret, P., "Resonantly induced refractive index changes in Yb-doped fibers: the origin, properties and application for all-fiber coherent beam combining," *Frontiers in Guided Wave Optics and Optoelectronics*, 209-234 (2010).

[8] Wang, K., Horton, N. G., Charan, K., and Xu, C., "Advanced fiber soliton sources for nonlinear deep tissue imaging in biophotonics," IEEE Journal of Selected Topics in Quantum Electronics, 20(2), 50-60 (2013).

[9] Stoliarov, D. A., Itrin, P. A., Ribenek, V. A., Korobko, D. A., & Fotiadi, A. A., "Linear cavity fiber laser harmonically mode-locked with SESAM," *Laser Physics Letters*, *17*(10) 105102 (2020).

[10] Rissanen, J., Korobko, D. A., Zolotovsky, I. O., Melkumov, M., Khopin, V. F., and Gumenyuk, R., "Infiltrated bunch of solitons in Bi-doped frequency-shifted feedback fibre laser operated at 1450 nm," *Scientific reports*, *7*(1), 1-10 (2017).

[11] Bello-Jiménez, M., Hernández-Escobar, E., Camarillo-Avilés, A., Pottiez, O., Díez, A., and Andrés, M. V., "Actively mode-locked all-fiber laser by 5 MHz transmittance modulation of an acousto-optic tunable bandpass filter," Laser Physics Letters, 15(8), 085113 (2018).

[12] Korobko, D. A., Gumenyuk, R., Zolotovskii, I. O., and Okhotnikov, O. G., "Multisoliton complexes in fiber lasers," *Optical Fiber Technology*, *20*(6), 593-609 (2014).

[13] Aleshkina, S. S., Fedotov, A., Korobko, D., Stoliarov, D., Lipatov, D. S., Velmiskin, V. V., and Likhachev, M. E., "All-fiber polarization-maintaining mode-locked laser operated at 980 nm," *Optics letters*, *45*(8), 2275-2278 (2020).

[14] Gumenyuk, R., Korobko, D. A., Zolotovsky, I. O., and Okhotnikov, O. G., "Role of cavity dispersion on soliton grouping in a fiber lasers," *Optics express*, *22*(2), 1896-1905 (2014).

[15] Korobko, D. A., Stoliarov, D. A., Itrin, P. A., Odnoblyudov, M. A., Petrov, A. B., and Gumenyuk, R. V., "Harmonic mode-locking fiber ring laser with a pulse repetition rate up to 12 GHz," *Optics & Laser Technology*, *133*, 106526 (2021).

[16] Gumenyuk, R. V., Korobko, D. A., and Zolotovskii, I. O., "Stabilization of passive harmonic mode locking in a fiber ring laser, *Optics Letters*, *45*(1), 184-187 (2020).

[17] Boivinet, S., Lecourt, J. B., Hernandez, Y., Fotiadi, A. A., Wuilpart, M., and Mégret, P., "All-Fiber 1-□m PM Mode-Lock Laser Delivering Picosecond Pulses at Sub-MHz Repetition Rate," *IEEE Photonics Technology Letters*, *26*(22), 2256-2259 (2014).

[18] López-Mercado, C. A., Spirin, V. V., Escobedo, J. B., Lucero, A. M., Mégret, P., Zolotovskii, I. O., & Fotiadi, A. A., "Locking of the DFB laser through fiber optic resonator on different coupling regimes," *Optics Communications*, *359*, 195-199 (2016).

[19] Haus, H. A. "Mode-locking of lasers," IEEE Journal of Selected Topics in Quantum Electronics, 6(6), 1173-1185 (2000).

[20] Brabec, T., Spielmann, C., Curley, P. F., and Krausz, F., "Kerr lens mode locking," Optics letters, 17(18), 1292-1294 (1992).

[21] Ilday, F. Ö., Wise, F. W., and Sosnowski, T., "High-energy femtosecond stretched-pulse fiber laser with a nonlinear optical loop mirror," Optics letters, 27(17), 1531-1533 (2002).

[22] Matsas, V. J., Newson, T. P., Richardson, D. J., and Payne, D. N., "Self-starting, passively mode-locked fibre ring soliton laser exploiting non-linear polarisation rotation," Electronics Letters, 28(15), 1391-1393 (1992).

[23] Chen, C. J., Wai, P. K. A., and Menyuk, C. R., "Soliton fiber ring laser," Optics letters, 17(6), 417-419 (1992).

[24] Korobko, D. A., Rastogi, V., Sysoliatin, A. A., and Zolotovskii, I. O., "Generation of 2 μm radiation due to single-mode fibers with longitudinally varying diameter," *Optical Fiber Technology*, *47*, 38-42 (2019).

[25] Isomaki, A., Vainionpaa, A. M., Lyytikainen, J., and Okhotnikov, O. G., "Semiconductor mirror for optical noise suppression and dynamic dispersion compensation," IEEE journal of quantum electronics, 39(11), 1481-1485 (2003).

[26] Okhotnikov, O., Grudinin, A., and Pessa, M., "Ultra-fast fibre laser systems based on SESAM technology: new horizons and applications," New journal of physics, 6(1), 177 (2004).

[27] Zolotovskii, I. O., Korobko, D. A., Gumenyuk, R. V., and Okhotnikov, O. G., "Generation of bound states of pulses in a soliton laser with complex relaxation of a saturable absorber," *Quantum Electronics*, *45*(1), 26 (2015).

[28] Zhao, C., Zhang, H., Qi, X., Chen, Y., Wang, Z., Wen, S., and Tang, D., "Ultra-short pulse generation by a topological insulator based saturable absorber," Applied Physics Letters, 101(21), 211106 (2012).

[29] Bao, Q., Zhang, H., Wang, Y., Ni, Z., Yan, Y., Shen, Z. X., and Tang, D. Y., "Atomic-layer graphene as a saturable absorber for ultrafast pulsed lasers," Advanced Functional Materials, 19(19), 3077-3083 (2009).

[30] Chernysheva, M., Rozhin, A., Fedotov, Y., Mou, C., Arif, R., Kobtsev, S. M., and Turitsyn, S. K., "Carbon nanotubes for ultrafast fibre lasers," *Nanophotonics*, *6*(1), 1-30 (2017).

[31] Kbashi, H. J., Sergeyev, S. V., Al-Araimi, M., Rozhin, A., Korobko, D., and Fotiadi, A., "High-frequency vector harmonic mode locking driven by acoustic resonances," *Optics letters*, *44*(21), 5112-5115 (2019).

[32] Huang, L., Zhang, Y., & Liu, X. (2020). Dynamics of carbon nanotube-based mode-locking fiber lasers. Nanophotonics, 9(9), 2731-2761. doi: 10.1515/nanoph-2020-0269

[33] Wang, J., Chen, Y., and Blau, W. J., "Carbon nanotubes and nanotube composites for nonlinear optical devices," Journal of Materials Chemistry, 19(40), 7425-7443 (2009).

[34] Avouris, P., Freitag, M., and Perebeinos, V., "Carbon-nanotube photonics and optoelectronics," Nature photonics, 2(6), 341-350 (2008).

[35] Martinez, A., and Sun, Z., "Nanotube and graphene saturable absorbers for fibre lasers," Nature Photonics, 7(11), 842-845 (2013).

[36] Gumenyuk, R., Okhotnikova, E. O., Filippov, V., Korobko, D. A., Zolotovskii, I. O., and Guina, M., "Fiber lasers of Prof. Okhotnikov: review of the main achievements and breakthrough technologies," *IEEE Journal of Selected Topics in Quantum Electronics*, *24*(3), 1-14 (2017).

[37] Chernov, A. I., Obraztsova, E. D., and Lobach, A. S., "Optical properties of polymer films with embedded single-wall carbon nanotubes," Physica status solidi (b), 244(11), 4231-4235 (2007).

[38] Solodyankin, M. A., Obraztsova, E. D., Lobach, A. S., Chernov, A. I., Tausenev, A. V., Konov, V. I., and Dianov, E. M., "Mode-locked 1.93 μm thulium fiber laser with a carbon nanotube absorber," Optics letters, 33(12), 1336-1338 (2008).

[39] Steinberg, D., Zapata, J. D., de Souza, E. A. T., and Saito, L. A., "Mechanically exfoliated graphite onto D-shaped optical fiber for femtosecond mode-locked erbium-doped fiber laser," Journal of Lightwave Technology, 36(10), 1868-1874 (2018).

[40] Luo, Z. C., Liu, M., Liu, H., Zheng, X. W., Luo, A. P., Zhao, C. J., and Xu, W. C., "2 GHz passively harmonic mode-locked fiber laser by a microfiber-based topological insulator saturable absorber," Optics Letters, 38(24), 5212-5215 (2013).

[41] Rehan, M., Kumar, G., Rastogi, V., Korobko, D. A., and Sysolyatin, A. A., "Compression of femtosecond pulses in a wide wavelength range using a large-mode-area tapered fiber," *Laser Physics*, *29*(2), 025104 (2019).

[42] Sui, Y., Gokhale, V. J., Shenderova, O. A., McGuire, G. E., and Rais-Zadeh, M., "A thin-film infrared absorber using CNT/nanodiamond nanocomposite," MRS Online Proceedings Library, 1452(1), 8-13 (2012).

[43] Song, Y. W., Morimune, K., Set, S. Y., and Yamashita, S., "Polarization insensitive all-fiber mode-lockers functioned by carbon nanotubes deposited onto tapered fibers," Applied physics letters, 90(2), 021101 (2007).

[44] Kieu, K., and Mansuripur, M., "Femtosecond laser pulse generation with a fiber taper embedded in carbon nanotube/polymer composite," Optics letters, 32(15), 2242-2244 (2007).

[45] Xu, B., Omura, M., Takiguchi, M., Martinez, A., Ishigure, T., Yamashita, S., and Kuga, T., "Carbon nanotube/polymer composite coated tapered fiber for four wave mixing based wavelength conversion," Optics express, 21(3), 3651-3657 (2013).

[46] Martinez, A., Al Araimi, M., Dmitriev, A., Lutsyk, P., Li, S., Mou, C., and Turitsyn, S., "Low-loss saturable absorbers based on tapered fibers embedded in carbon nanotube/polymer composites," APL Photonics, 2(12), 126103 (2017).

[47] Agrawal, G. P. (2020). Applications of nonlinear fiber optics. Academic press.

[48] Labunov, V. A., Tabulina, L. V., Komissarov, I. V., Rusal'skaya, T. G., Kashko, I. A., Shulitskii, B. G., and Pavlov, A. A., "Effect of Liquid-Phase Oxidative Treatments on the Purity, Hydrophilicity, and Structure of Single-Wall Carbon Nanotubes and on the Electrical Conductivity of Their Arrays," Russian Journal of Applied Chemistry, 93(5), 679-690 (2020).

[49] Zolotovskii, I. O., Korobko, D. A., and Lapin, V. A., "Modulation instability and short-pulse generation in media with relaxing Kerr nonlinearity and high self-steepening," *Quantum Electronics*, *44*(1), 42 (2014).

[50] Kataura, H., Kumazawa, Y., Maniwa, Y., Umezu, I., Suzuki, S., Ohtsuka, Y., and Achiba, Y., "Optical properties of single-wall carbon nanotubes," Synthetic metals, 103(1-3), 2555-2558 (1999).

[51] Sobon, G., Duzynska, A., Świniarski, M., Judek, J., Sotor, J., and Zdrojek, M., "CNT-based saturable absorbers with scalable modulation depth for Thulium-doped fiber lasers operating at 1.9 μm," Scientific Reports, 7, 45491 (2017).

[52] Lee, C. C., Miller, J. M., and Schibli, T. R., "Doping-induced changes in the saturable absorption of monolayer graphene," Applied Physics B, 108(1), 129-135 (2012).

[53] Wang, J., Jiang, Z., Chen, H., Li, J., Yin, J., Wang, J., and Ruan, S., "High energy soliton pulse generation by a magnetron-sputtering-deposition-grown MoTe 2 saturable absorber," Photonics Research, 6(6), 535-541 (2018).

[54] Yin, J., Zhu, F., Lai, J., Chen, H., Zhang, M., Zhang, J., and Ruan, S., "Hafnium sulfide nanosheets for ultrafast photonic device," Advanced optical materials, 7(5), 1801303 (2019).

[55] He, J., Tao, L., Zhang, H., Zhou, B., and Li, J., "Emerging 2D materials beyond graphene for ultrashort pulse generation in fiber lasers," *Nanoscale*, *11*(6), 2577-2593 (2019).

[56] Jiang, T., Yin, K., Wang, C., You, J., Ouyang, H., Miao, R., and Zhang, H., "Ultrafast fiber lasers mode-locked by two-dimensional materials: review and prospect," *Photonics Research*, *8*(1), 78-90 (2020).

[57] Ma, P. F., Lin, W., Zhang, H. N., Xu, S. H., and Yang, Z. M., „Nonlinear absorption properties of Cr2Ge2Te6 and its application as an ultra-fast optical modulator," *Nanomaterials*, *9*(5), 789 (2019).

[58] Kang, Z., Liu, M., Tang, C., Xu, X., Jia, Z., Qin, G., and Qin, W., "Microfiber coated with gold nanorods as saturable absorbers for 2 μm femtosecond fiber lasers," *Optical Materials Express*, *8*(12), 3841-3850 (2018).